



# A Digital Platform for Simulating the Accurate Detectability of Overactive Parathyroid Glands in SPECT/CT Imaging

Ayşegül ORAL and Albert GÜVENİŞ

Institute of Biomedical Engineering  
Boğaziçi University  
İstanbul, TURKEY

aysegul.oral@outlook.com.tr, guvenisis@gmail.com

**Abstract**—Reliable detection of overactive parathyroid glands is still a currently unmet need in preparing minimally invasive surgical interventions. Compared to physical phantom studies, computer simulation has the potential to explore a large number of parameters with higher flexibility at a lower cost. In this study, a digital platform was developed to optimize the parathyroid SPECT/CT imaging protocols. The SIMIND platform was used for Monte Carlo simulation. The Zubal digital phantom was modified in order to include a small spherical artificial adenoma. Contrast-to-noise ratio was selected as a surrogate measure of lesion detectability. Best CNR values were determined using different collimators. Lesion detectability was analyzed based on the assumption that the thyroid activity was mostly vanished in the subtraction or dual phase protocol. The results showed that highest resolution-collimators yielded the highest CNR values. Future work will use this platform in order to search higher detectability levels with other acquisition and reconstruction parameters for different camera brands.

**Keywords**—SPECT; parathyroid scintigraphy; Monte-Carlo simulation; optimization.

## I. INTRODUCTION

Patients suffering from Primary hyperparathyroidism (PHPT) have overactive parathyroid glands that produce an elevated amount of Parathormon (PTH). This leads to high amounts of calcium in the blood and urine. In time, this condition can lead to osteoporosis, kidney stones and kidney function deterioration [1]. A common cause is an adenoma on a single gland but can also be caused by adenomas on multiple glands (about 20% of PHPT patients). An adenoma makes the gland overactive.

Minimally invasive surgery which has recently become common can decrease complications. The treatment outcome can be immediately verified by measuring the parathyroid hormone concentration which should be reduced by 50% or more in a time interval of 10 min after removal of the adenoma(s).

Before undertaking minimally invasive surgery, it is imperative and critical to detect and precisely localize the adenomas. This is carried out by the use of various available medical imaging procedures, including MRI [2,3], CT [4,5],

ultrasound [6,7] or PET [8,9]. SPECT is known to offer excellent functional and molecular imaging possibilities. However, its image quality is compromised by physical degradations. It is therefore important to improve image quality by conducting optimization studies.

Tc-99m Sestamibi is known to be absorbed by both the thyroid and adenomas whereas I-123 sodium iodide is retained only in the thyroid. In the dual phase procedure, the fact that the Tc-99m Sestamibi washes out faster from the thyroid than the adenomas is utilized in order to isolate the adenomas [10]. A review of the studies comparing SPECT/CT, SPECT and planar imaging is given in [11].

SPECT imaging presents several challenges due to the high noise and low spatial resolution in nuclear medicine imaging in particular for small lesions. It is therefore important to optimize image quality with respect to data acquisition and image reconstruction parameters. Some studies addressed the fundamental issue of optimal parameter value selection for data acquisition and reconstruction. In one study [12], a phantom study was undertaken. In another study [13] a protocol optimization was undertaken with real patients. Both types of studies are important for determining the best parameters. However, optimization studies with real phantoms or patients are costly and do not address the issue of using different scanning equipment. Furthermore, the studies [12,13] relied mostly on subjective criteria or a limited contrast measurement. These studies tend to be even lengthier with increasing number of parameters to be optimized.

In order to tackle these difficulties, in this study, we approach the optimization problem using Monte Carlo simulation which offers a flexible platform for experimenting with protocols [14,15]. In this initial study, the effect of the type of collimator on detectability is studied. Contrast-to-noise ratio (CNR) is used as a surrogate measure to evaluate detectability.

To our knowledge, this is the first time that Monte Carlo simulation has been used for studying parathyroid SPECT imaging or comparing different acquisition conditions. This was performed as an extension of an initial work [16] where only one single condition was studied. Establishing a simulation platform may help us answer many questions as new quantification techniques emerge and more parameters are



added to the optimization process. The sensitivity of optimal protocols to different scanners can also be addressed.

## II. METHODS

The general approach taken in this work can be summarized as follows: Build a digital antropomorphic phantom using previous physical phantom studies in the literature based on the SIMIND Monte Carlo Simulation Package and compare the detectability of adenomas using contrast-to-noise ratios.

### A. General

In order to acquire a parathyroid scintigraphy image, it is assumed that the thyroid is eliminated either by the use of subtraction or the dual phase method where the thyroid activity is washed out. In either case, residuals of the thyroid activity can decrease the visibility of the adenoma. However, in this study the aim is not to compare the two protocols but improve the detectability of the adenoma by a judicious choice of the collimator. It goes without saying that residual thyroid activity will hamper the detectability of the adenoma however our interest is to increase the detectability of the adenoma in general. How well dual phase and subtraction techniques can remove the thyroid is another issue. According to the guidelines, an average recommended total acquisition time is 25 minutes and the acquired image matrix should be at least of size 128x128 [10]. Iterative reconstruction algorithms give better performance. In iterative reconstruction algorithms, as the iteration number increases, better contrast values may appear but image noise increases also.

### B. Monte Carlo Simulation

Monte Carlo Simulation is a technique where a random number generator is used to simulate stochastic processes. In SPECT imaging, it can be used to study the causes of degradation in images.

In this work, the SIMIND simulation platform has been adopted [17] which has been validated in several studies [14, 18, 19, 20]. The entire code is written in Fortran-90. Simulation was conducted using the commands described in [17]. First the CHANGE program was activated in order to set the parameters of the simulation that include phantom activity, acquisition parameters and detector properties. Then, simulation was performed using the SIMIND command and reconstruction was performed based on the CASTOR software that can be called within the SIMIND package. Noise was added using the ImageJ software. The following sections describe the parameters used during simulations and image reconstruction.

### C. Phantom Modeling

In order to carry out a Monte Carlo simulation corresponding to the real human anatomy, an antropomorphic phantom was selected. In this study the Zubal torso phantom (with no arms or legs attached) was simulated with the SIMIND Monte Carlo Simulation Program [17,21]. The slice resolution was chosen 128x128 pixels [10, 12] as the Zubal phantom's original structure. Pixel size and slice thickness were defined 0.24 cm per pixel in the x, y and z plane with the use of the SIMIND.

A parathyroid adenoma was considered and modeled as a sphere behind the thyroid gland and filled with 99mTc with a

density of 0.5 MBq/cc [10]. 99mTc concentration ratio was chosen approximately 16:1 for the parathyroid adenoma and background models [12]. The adenoma's radius was selected as 0.38 cm [5].

### D. Data Acquisition Modeling

In this study, acquisition time was 33 seconds per projection. 10 seconds per projection was assumed.

Every simulation case had an attenuation correction file. Simulations were performed with parallel whole collimators. According to the last Finnish hospitals' survey, only 28% of the parathyroid imaging has been performed by pinhole collimators [23].

### E. Collimators

The Siemens SymbiaIntevo Low Energy High Resolution, Medium Energy Low Penetration and Low Energy Ultra High Resolution (LEHR, MELP and LEUHR) collimators were studied. Camera specifications change from device to device. These parameters can be altered in the SIMIND Change Program. 180° detector configuration and the step-and-shoot method (48 views total) were used. Septal penetration option was enabled in SIMIND.

### F. Image Corrections and Reconstruction

An important type of image degradation is caused by attenuation which is caused by both absorption and scattering of photons inside the object to be imaged. The human body is an attenuating medium and therefore the image is highly influenced. If not removed, the attenuation effects have the potential to create artifacts and degrade the diagnostic accuracy. In this study attenuation correction was implemented using SIMIND and CASTOR and was kept on for all simulations. Scatter correction was not included.

8 iterations with 8 subsets were chosen as reconstruction parameters. All simulated projections were reconstructed using the Castor reconstruction package.

### G. SIMIND Parameters

SPECT imaging parameters can be divided into three main categories as device, acquisition and processing parameters. The effect of collimator types, various camera brands, and crystal thickness were studied under the title of device parameters.

Acquisition parameters included matrix size, number of counts, energy window, number of projections, projection time. Processing parameters comprised correction options, the number of iterations and the number of subsets. The SIMIND parameters were set according to datasheets provided by manufacturers [24].

### H. Statistical Analysis and Lesion Detectability

For the region of interest, the pixels belonging to the synthetic adenoma were selected for statistical calculations after the reconstruction process. The background was selected from the area outside the adenoma. The mean pixel value and standard deviation were calculated for the adenoma and the background region of interest using the ImageJ software.

The ratio of the difference between the average counts in the two areas to the counts in the background was used to compute the contrast. The second parameter that is used for statistical evaluation is noise. CNR (contrast to noise ratio) is the critical parameter for lesion detectability.

Contrast values were calculated using the equation (1):

$$C = (\mu_A - \mu_B) / \mu_B \quad (1)$$

where  $\mu_A$  is the mean value of the counting rate of the adenoma and  $\mu_B$  is the mean value of the counting rate of the background region of interest. In this work, CNR values were calculated using the equation (2):

$$CNR = (\mu_A - \mu_B) / \sigma(\mu_B) \quad (2)$$

where  $\sigma(\mu_B)$  is the standard deviation of the mean voxel value of the background.

### III. RESULTS

The following gives the results obtained for the different collimators of the Siemens Camera. Both CNR values and corresponding images were included in order to allow visual assessment.

TABLE I. CNR RESULTS FOR THE SIEMENS SYMBIA GAMMA CAMERA SIMULATIONS WITH 3 COLLIMATORS FOR 8 ITERATIONS, 8 SUBSETS AND WITH ATTENUATION CORRECTION ONLY

CNR Results with Poisson Noise						
ID	Collimator	adenoma	background	contrast	sd of bg mean	CNR
1p	LEHR	506	340	0,49	75,6	2,19
2p	MELP	1072	1164	-0,08	154	-0,6
3p	LEUHR	332	166	1	47	3,53

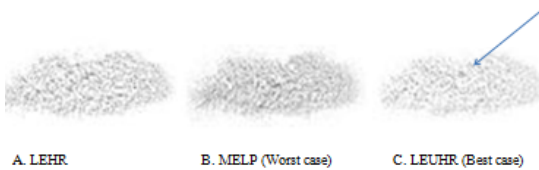


Figure 1. Transversal images for Siemens collimators LEHR, LEUHR and MELP. A. LEHR, (CNR=2,19) B. MELP, (CNR=-0,60). C. LEUHR, (CNR=3,53). The adenoma is clearly visible in C (LEUHR). MELP is not used in dual phase imaging but can be considered for subtraction imaging protocol where I-123 is additionally used.

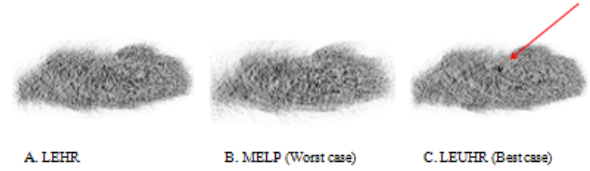


Figure 2. LEUHR and MELP when no noise is added. A. LEHR, (Contrast=0,24) B. MELP, (Contrast=0,13) C. LEUHR, (Contrast=0,66). The adenoma is clearly visible in C (LEUHR).

Table 1 and Figure 1 give the results for the Siemens Symbia Gamma Camera Simulations. Arrows point to the adenoma. It can be seen that the LEUHR gives the best detectability both quantitatively (CNR) and visually. Note that the number of counts in the projection data was found similar to the literature [22]. Results for the case, when no noise is added, can be seen in Figure 2.

### IV. DISCUSSION

This study aimed to first develop a computer simulation platform for parathyroid SPECT imaging and second, find the best collimator for a specific camera while the evaluation criterion was CNR.

CNR was found to be the highest for the LEUHR collimator (Table 2, Figure 1).

The higher-resolution collimator yielded better results, which can be explained by the fact that the lesion profile is less spread out, has a higher peak and therefore the contrast is higher. Although high-resolution collimators are less sensitive, the reduction in counts and therefore increase in noise did not affect the CNR as much as the increase in the contrast. With the use of lower resolution collimators, the lesion profile tends to spread out and therefore the contrast is significantly reduced. We can therefore say that the tradeoff between sensitivity and resolution worked for the advantage of the resolution.

With lower resolution collimators, either sensitivity is increased (larger holes) or penetration is decreased (larger septa). With increased sensitivity, Poisson noise is decreased. With decreased penetration, contrast is increased.

#### A. Comparison with previously reported findings

To the best of our knowledge, there are no phantom studies on the optimization of dual phase parathyroid SPECT imaging protocols. According to this study, the very high-resolution collimators seem to perform better for parathyroid imaging with Tc-99m Sestamibi. This result is similar to findings of the phantom study in [12] conducted for subtraction parathyroid scintigraphy.

Note that this study was based on CNR while the cited phantom study in [12] used contrast and a subjective visibility index. CNR is an objective quantitative measure of detectability using noise as well as contrast levels. Patient studies are important for validating protocols but lack ground truth information. Computer simulation allows us to study the effect



of parameters on detectability in a quantitative and efficient way. There is access to a large number of simulation variable results.

Since the focus was on the detectability of the adenoma, assuming a complete removal of the thyroid, the results may be extended to both protocols (dual phase and subtraction). In fact our results agree with the results in [12] where a subtraction protocol was investigated. The comparison of these two protocols is another research topic.

#### B. Limitations and Future Work

It was assumed that the thyroid activity was completely washed out on the delayed image.

Parameters such as scatter correction, number of counts, and other reconstruction and processing parameters have not been considered here. Other types of cameras may also be studied in the future.

#### V. CONCLUSIONS

An antropomorphic digital phantom was built for the optimization of the parathyroid imaging using Monte Carlo Simulation for the first time. The platform offers flexibility and efficiency in implementing optimization strategies using different camera types and a larger number of both acquisition and processing parameters. It may also shed light to the relationships between parameters and the performance figures.

The initial results show that higher-resolution collimators yield the best detectability. The platform will be used to design new experiments that will include further acquisition and processing parameters.

#### REFERENCES

- [1] Walker, Marcella D., and Shonni J. Silverberg. "Primary hyperparathyroidism." *Nature Reviews Endocrinology* 14, no. 2, 115, 2018.
- [2] Merchavy, S., Luckman, J., Guindy, M., Segev, Y., & Khafif, A. "4DMRI for the localization of parathyroid adenoma: a novel method in evolution." *Otolaryngology--Head and Neck Surgery*, 154(3), 446-448, 2016.
- [3] Argirò, R., Diacinti, D., Sacconi, B., Iannarelli, A., Diacinti, D., Cipriani, C., ... & Pepe, J. Diagnostic accuracy of 3T magnetic resonance imaging in the preoperative localisation of parathyroid adenomas: comparison with ultrasound and 99mTc-sestamibi scans. *European radiology*, 28(11), 4900-4908, 2018.
- [4] Vu, T. H., D. Schellingerhout, N. Guha-Thakurta, J. Sun, W. Wei, S. C. Kappadth, N. Perrier et al. "Solitary Parathyroid Adenoma Localization in Technetium Tc99m Sestamibi SPECT CT and Multiphase Multidetector 4D CT." *American Journal of Neuroradiology* 40(1), 142-149, 2019.
- [5] Czarniecki, Caroline A., Paul F. Einsiedel, Pramit M. Phal, Julie A. Miller, Meir Lichtenstein, and Damien L. Stella. "Dynamic CT for Parathyroid Adenoma Detection: How Does Radiation Dose Compare With Nuclear Medicine?." *American Journal of Roentgenology* 210, no. 5, 1118-1122, 2018.
- [6] Leung, V., Nishtala, S., & Oxtoby, J. Diagnostic accuracy of ultrasound and dual-isotope scintigraphy for parathyroid adenoma localisation. *Clinical Radiology*, 72, S10, 2017.
- [7] Stern, S., Tzelnick, S., Mizrachi, A., Cohen, M., Shpitzer, T., & Bachar, G. Accuracy of neck ultrasonography in predicting the size and location of parathyroid adenomas. *Otolaryngology--Head and Neck Surgery*, 159(6), 968-972, 2018.
- [8] Parvinian, Ahmad, Erica L. Martin-Macintosh, Ajit H. Goenka, Jolanta M. Durski, Brian P. Mullan, Brad J. Kemp, and Geoffrey B. Johnson.

- "11C-Choline PET/CT for Detection and Localization of Parathyroid Adenomas." *American Journal of Roentgenology* 210, no. 2, 418-422, 2018.
- [9] Prabhu, M., Damle, N., Kumari, G., Tripathi, M., Bal, C., Arora, G. E. E. T. A. N. J. A. L. I., ... & Kandasamy, D. A pilot study to assess the role of early dynamic PET/CT with 18F-Fluorocholine in imaging of parathyroid adenomas. *Journal of Nuclear Medicine*, 59(supplement 1), 1326-1326, 2018.
- [10] Greenspan BS, Dillehay G, Intenzo C, et al. SNM practice guideline for parathyroid scintigraphy 4.0. *J Nucl Med Technol.*; 40(2): 111-118,doi: 10.2967/jnmt.112.105122, indexed in Pubmed: 22454482, 2012.
- [11] Wei WJ, Shen CT, Song HJ, et al. "Comparison of SPET/CT, SPET and planarimaging using 99mTc-MIBI as independent techniques to support minimallyinvasiveparathyroidectomy in primary hyperparathyroidism: A meta-analysis." *Helv J Nucl Med.*; 18(2): 127-135, doi: 10.1967/s002449910207 indexed in Pubmed: 26187212, 2015.
- [12] Tunninen, V., Kauppinen, T., & Eskola, H. Optimization of 99m Tc-sestamibi/123 I subtraction SPECT/CT protocol for parathyroid scintigraphy. In *EMBECC & NBC Springer*, Singapore, 847-851, 2017.
- [13] Mallak, N., Kashyap, A., Murguia, J., Sugg, S., & Graham, M. "Optimization of Parathyroid Imaging for Small Adenomas". *Journal of Nuclear Medicine*, 58(supplement 1), 100-100, 2017.
- [14] Mahler, E., Sundstrom, T., Axelsson, J., & Larsson, A. Detecting Small Liver Tumors With  $^{111}\text{In}$ -Pentetreotide SPECT—A Collimator Study Based on Monte Carlo Simulations. *Ieee transactions on nuclear science*, 59(1), 47-53, 2011.
- [15] Roshan, H. R., Mahmoudian, B., Gharepapagh, E., Azarm, A., & Islamian, J. P. Collimator and energy window optimization for 90Y bremsstrahlung SPECT imaging: A SIMIND Monte Carlo study. *Applied Radiation and Isotopes*, 108, 124-128, 2016.
- [16] Oral, A., Guvenis, A. "A Monte Carlo Simulation of Parathyroid SPECT Imaging", *International Congress on Biological and Medical Science*, Niğde,Turkey, 7, 2018.
- [17] Ljungberg, M., "The simind monte carlo program manual," 2017. Available: [http://www2.msf.lu.se/simind/download/Simind\\_manual.pdf](http://www2.msf.lu.se/simind/download/Simind_manual.pdf).
- [18] Ejeh, John E., Johan A. van Staden, and Hanlie du Raan. "Validation of SIMIND Monte Carlo Simulation Software for Modelling a Siemens Symbia T SPECT Scintillation Camera." In *World Congress on Medical Physics and Biomedical Engineering 2018*, pp. 573-576. Springer, Singapore, 2019.
- [19] Gear, Jonathan I., Jan Taprogge, Owen White, and Glenn D. Flux. "Characterisation of the attenuation properties of 3D-printed tungsten for use in gamma camera collimation." *EJNMMI physics* 6, no. 1 (2019): 1.
- [20] Karamat, Muhammad I., and Troy H. Famcombe. "Simultaneous 99m tc/111 in spect reconstruction using accelerated convolution-based forced detection montecarlo." *IEEE Transactions on Nuclear Science* 62, no. 5 2085-2095, 2015.
- [21] Ljungberg M, Strand S-E, King MA. *Monte Carlo Calculations in Nuclear Medicine Applications in Diagnostic Imaging*. 1st ed. (Ljungberg M, Strand S-E, King MA, eds.). Bristow and Philadelphia: IOP Publishing; 1995.
- [22] Chen, H., Sippel, R. S., & Schaefer, S. "The effectiveness of radioguided parathyroidectomy in patients with negative technetium Tc 99m-Sestamibi scans". *Archives of Surgery*, 144(7), 643-648, 2009.
- [23] Klingensmith, W. C., Koo, P. J., Summerlin, A., Fehrenbach, B. W., Karki, R., Shulman, B. C., ... & McIntyre, R. C. Parathyroid imaging: the importance of pinhole collimation with both single-and dual-tracer acquisition. *Journal of nuclear medicine technology*, 41(2), 99-104, 2013.
- [24] Siemens symbia t series system specifications, 2013. Available: <https://3.imimg.com/data3/AC/PC/MY-13438971/gamma-camera.pdf>.